RSC Advances

ROYAL SOCIETY OF CHEMISTRY

www.rsc.org/advances

Superhydrophobic and anti-corrosion Cu microcones/Ni-W alloy coating fabricated by electrochemical approaches

Fengtian Hu[a], Penghui Xu[a], Haozhe Wang[b], Anmin Hu*[a], Ming Li*[a]

[a]*State Key Laboratory of Metal Matrix Composites, Key Laboratory for Thin Film and Microfabrication Technology of the Ministry of Education, School of Materials Science and engineering, Shanghai Jiao Tong University,Shanghai 200240,People's Republic of China*

[b]*Department of Mechanics Engineering，Massachusetts Institute of Technology.*

Abstract: In this work, we present a simple method for fabricating the microstructured Cu / Ni-W alloy coating by combining electroless and electro deposition. Field emission scanning electron microscopy (FESEM) results show that a layer of Ni-W alloy has uniformly covered on the conical surface of Cu microcone arrays, forming a multilayer coating. Tafel curve shows the prominent anti - corrosion property of the as-deposited Ni-W film. Wettability results reveal that the water contact angles can be increased from 106° to 153.2° by adjusting the electrodeposition time of Ni-W layer. The liquid-solid-air contact mode between the superhydrophobic Ni-W hemisphere decorated Cu microcone array and the water drop is briefly discussed. This work also showed the potential which can be used in a wide range of applications, such as the commercial production of anti-wetting and anti-corrosion

* Corresponding author Tel: +86 021 34202748
Email address: huanmin@sjtu.edu.cn

* Corresponding author Tel: +86 021 34202748
Email address: mingli90@sjtu.edu.cn

devices.

1.Introduction

Wettability is an important feature of a solid surface, which is determined by force balance between adhesive and cohesive forces. This property is usually described by measuring the contact angle, which is formed in the contact interface between the liquid and solid surface. Usually, the surface which contact angle is greater than 150 degrees is defined as the superhydrophobic surface. Superhydrophobic surface has various functional applications in engineering materials, involving space, construction, automotive, aviation, microelectronics and transportation industry. Researches on the surface of engineering materials are of great significance to the superhydrophobic surface and its applications in industry. The wetting properties of the surface of engineering materials determine the adhesion of the materials. Superhydrophobicity possesses broad prospects for application in self - cleaning,[1] fluid drag reduction,[2] anticorrosive,[3,4] oil-water separation[5-7] and so on. Therefore, it has gained the extensive concern of the researchers in recent years.[1,8,9]

Structures at the nanometer and the micrometer scale are required to entrap air below water droplets and thus reduce the liquid-solid contact and cause superhydrophobicity. Jiang *et al*. reported that the surface of the lotus leaf is covered with dual-scale hierarchical structured protuberances.[10] Zhang *et al*. reported that the superhydrophobic nanoporous polydivinylbenzene materials are synthesized.[11] Mo *et al*.exhibited that the self-cleaning and superhydrophobicity can be realized on the Au-coated Ni nanocone arrays surface.[12]

As a commonly used material, compared with other metals and alloys, copper and copper alloy has more excellent electrical conductivity, thermal conductivity and electricity resistance transition. As a strategic metal material, it has the extremely widespread application in many fields. In our previous work, Zhang[13] successfully fabricated dense copper microcones arrayed structure by electroless plating with crystal modification. However, Cu has a high affinity to oxygen and a soft texture, which lead to inferior device performance and failure. Therefore, one of the biggest challenges of Cu application is the prevention of Cu oxidation and corrosion.[14] As an essential engineering material, Ni-W alloy has an excellent high-temperature corrosion resistance and low permeability to diffusion.[15-17] When Ni-W alloy coating was deposited on Cu surface, it can protect Cu surface from corrosion and scratch.The addition of W to the Nickel film has attracted a great deal of attention in recent years, especially the Ni-W alloy film.[18,19] The W atoms in Ni and their segregation to grain boundaries make the alloy film more stable. Till now, there are few reports about the surface morphology and superhydrophobic mechanism of Cu microcones / Ni-W alloy coating.

In this work, we have prepared Cu / Ni-W multilayer coating with micro-posts arrayed surface by a facile two-step approach combining electroless with electro deposition. The micro-posts morphology after surface modification shows excellent superhydrophobicity. Furthermore, the contact model between contact angle and surface morphology is briefly discussion. The synthesis processes of different layers (Cu and Ni-W) are expected to be appropriate for commercial applications.

2. Experiment

Cu microcone arrays (MCAs) / Ni-W alloy coating was fabricated by a two-step deposition method. Firstly, Cu plates were electrochemically degreased for 1 min, acid-cleaned with 20% HCl for 20 s and $PdCl_2$ activation for 60 s. After the pre-treatment, the copper microcone array was plated on the substrate in the bath solution by electroless deposition. The electrolyte was composed of analytical pure $CuSO_4 \cdot 5H_2O$ (0.03 mol/L), $NiSO_4 \cdot 6H_2O$ (0.0024 mol/L), $NaH_2PO_2 \cdot H_2O$ (0.24 mol/L), $Na_3C_6H_5O_7 \cdot 2H_2O$ (0.05 mol/L) and H_3BO_3 (0.50 mol/L) as well as crystallization modifier polyethylene glycol (5 ppm), which is referred to step one. The temperature was kept at 60°C and pH value was 8.5-9.0 (adjusted by 20% NaOH solution).

Subsequently, Ni-W (25 wt.%) alloy coating was electroplated on the as-prepared copper microcone-arrayed substrate at a constant current density of 10A/dm^2, which is referred to step two. The electrolyte for electro-plating of Ni-W alloy coating consisted of analytical pure $NiSO_4 \cdot 6H_2O$ (0.22 mol/L), $NaWO_4 \cdot 2H_2O$ (0.07 mol/L), $Na_3C_6H_5O_7 \cdot 2H_2O$ (0.5 mol/L), NH_4Cl (0.50 mol/L) and NaBr (0.15 mol/L), as previously reported.[20] The deposition time varied from 0.5 min to 2.5 min and the solution temperature was 60°C. The morphology of the deposits was studied by the scanning electronic microscope (SEM; FEI Sirion 200 HR FE-SEM). X-ray diffraction (XRD; Rigaku D/MAX-IIIA) was used to identify the phases from 20° to

95° with Cu Ka radiation (λ=0.15418 nm). Water contact angles (CA) were measured using a sensile drop method of an optical contact angle measuring device (OCA20) at ambient temperature. A drop of 3μL was placed on the surface, and each reported angle datum is calculated as the average of five measurements in different points on the sample. The electrochemical analysis was performed in a three electrode-system setup at CHI 660c electrochemical work station at room temperature in 3.5 wt% NaCl solution as the corrosive medium. X-ray fluorescent spectroscopy (XFS; Fsiherscope X-Ray XUL-XYm) measurements were carried out to measure the thickness of Ni-W layer. Each data in this study was an average of five measurements of different regions in order to achieve more precise data.

3.Results and discussions

3.1 Morphological observation

Fig.1 demonstrates the typical morphology of Cu MCAs deposit fabricated by electroless deposition. Cu MCAs are chemically deposited on the copper foil with a size of 2-4 μm in height and about 1 μm in bottom diameter. The copper deposits exhibit fine, dense, and uniform and typical cone shape. The tips of the MCAs are very sharp. This unique structure is closely related to the concentration and type of crystallization modifier which has been reported in our previous work.[21]

Fig. 2 shows the surface morphology of the electroless plated Cu MCAs before and after the deposition of Ni-W alloy coating with different deposition time. Fig. 2

(A) illustrates the typical cone structure. Fig.2 (B)-(F) reveal the structure evolution corresponding to different deposition time. With the increasing of the Ni-W alloy deposition time, the tips of Cu MCAs become less sharp. And the microcones are gradually transforming to hemisphere-structure. This trend is extremely obvious after deposition time mounting to 1.5 min (Fig. 2(D)), from which we can see that the gaps among the Cu MCAs are filled up and the surface is inclined to be smoothness. As the layer of Ni-W alloy deposit become thicker, the original Cu MCAs totally disappear and the surface is finally coated with tightly packed micro-hemispheres, as shown in Fig. 2 (F).

3.2 Influence of deposition time on thickness

The relationship between thickness of Ni-W alloy layer and plating time is illustrated in Fig.3. Under each condition, 5 specimens were tested for statistic accuracy. When specimens plated for 0.5 min, 1 min, 1.5 min, 2 min and 2.5 min, the average thicknesses of the five conditions are measured to be 0.73 μm, 1.43 μm, 2.15 μm, 2.88 μm and 3.59 μm, respectively. With deposition time increasing, the thickness of the Ni-W coating increases. The linear relationship between the thickness of Ni-W layer and depositing time accords with the following equation:

$$d = 1.43t \quad (1)$$

Where the symbol d represents the thickness and t is the depositing time.

3.3 XRD analysis

Fig.4 shows the X-ray diffraction pattern of Cu MCAs / Ni-W (25 wt.%.) alloy

coating, demonstrating the existence of both Cu and Ni-W alloy. Three strong diffraction peaks near the diffraction angles of 43°, 50° and 74° are in accordance with diffractions of Cu crystal face (111), (200) and (220) respectively, which can be indexed as face-centered cubic (fcc) Cu (JCPDS File No.040836), as shown Fig.4 (A). It is clearly seen from Fig. 4 (B) that it appears three peaks near 44.3°, 51.8° and 75.9°, indicating the formation of crystal structure. It is well acknowledged that three diffraction peaks of pure W are $2\theta_1 = 40.26°$, $2\theta_2 = 58.36°$, $2\theta_3 = 73.38°$ and that of pure Ni are $2\theta_1 = 44.62°$, $2\theta_2 = 51.94°$, $2\theta_3 = 76.14°$, corresponding to the diffractions of Ni crystal face (111), (200) and (220), which can be indexed as fcc Ni (JCPDS File No.040850). The result shows that the peak position and peak intensity of Ni-W alloy and pure Ni are extremely close, demonstrating that the alloy is a substitutional solid solution, in which Ni is the solvent and W is the solute. Since the W atom radius is larger than the radius of Ni atom, the Ni lattice expansion is caused by the formation of solid solution. It makes the interplanar spacing increase and the 2θ should be moved to the lower direction by the Prague formula, which is the same as the experimental results.

3.4 Microhardness

The vickers hardness of pure Cu is 369 Mpa far lower than that of Ni and W, while the vickers hardness of pure Ni and W are 638Mpa and 3430 Mpa respectively. Therefore, it can be inferred that the hardness value of Ni-W film on the surface of Cu MCAs is increased with the increase of the thickness of Ni-W film and the overall

hardness value of the substrate is increased.[22] The surface hardness of the substrate was measured with a Vickers hardness tester. With deposition time increasing, the hardness value of surface increases because of the thickness of Ni-W alloy increasing,as shown in Fig. 5. This can improve the texture of copper and prevent scratching.

3.5 Anti - corrosion property

Tafel curve is established to explain the anti - corrosion property. In Tafel region of the electrode curve, the relationship of corrosion potential and corrosion current density can be described in terms of the equation:

$$E = a + b \cdot log[I] \quad (2)$$

where the symbol E is the overpotential, I the corrosion current density, a and b are constant. It can be seen that the natural logarithm of current density is linear with the over potential in Tafel region. Therefore, the intersection of the corresponding E is the corrosion potential E_{corr} by the extension of the cathodic polarization curve and anodic polarization curve of the Tafel region and the corresponding I is the corrosion current density I_{corr}. The Tafel curves of the bare Cu MCAs and Cu MCAs coated Ni-W alloy film with the hemisphere-structure measured in 3.5 wt% NaCl solution are shown in Fig.6. The electrochemical analysis is recorded with a sweep rate of 0.01V/s from -0.4 V to 0.1 V of the open circuit potential. From the curves we can see the E_{corr} of Cu MCAs is -0.214 V while that of Cu MCAs coated 1.5 min Ni-W alloy film is -0.109 V, indicating that the E_{corr} of Cu MCAs coated Ni-W alloy surface is

more positive than the bare Cu MCAs substrate. Meanwhile, the I_{corr} also decreased from 10.73 μA/cm^2 to 0.85 μA/cm^2. Since I_{corr} is proportional to the etching rate, the corrosion resistance is enhanced after the corrosion rate of Ni-W alloy coating Cu MCAs decreasing. In addition, the I_{corr} of the Ni-W alloy surface is approximately 8% that of the bare Cu MCAs substrate. It can be concluded that the as-prepared Ni-W alloy surface has excellent corrosion resistance that can protect the bare Cu MCAs substrate from corrosion effectively. The superior corrosion resistance of Ni-W alloy film was due to preferential dissolution of Ni and formation of W rich film on the surface, which inhibited further corrosion.[23]

3.6 Superhydrophobicity and weather-resistance

The static contact angle was measured to evaluate the wettability of the Ni-W alloy coating. As shown in Fig. 7, the Cu MCAs surface shows a contact angle of 106°. The hydrophobicity of coating deposited with Ni-W alloy reaches a climax showing a contact angle of 153.2°. However, as the deposition of Ni-W alloy continues, the water contact angle of the surface reduced instead. In order to evaluate the effect of various corrosive solutions on the wettability of the Ni-W alloy coating (desposition time is 1.5 min), the water contact angles after immersion in solutions with different pH values for 2h have been measured (Fig. 8). The contact angle is larger than 150° when the pH is 1 or 14. Other conditions, like freezing 2h, 200°C 2h and 2 months (Fig. 8), were also shown to have little influence on the

superhydrophobicity.

Combining results above, it can be concluded that the superhydrophobicity of the resulting Cu MCAs surface must be closely correlative with the surface roughness. Liquids are assumed to only contact the sharp tips of the cones and air pockets are trapped beneath the liquid, which gives a composite state. In this state, the air parts of the surface can be considered completely non-wetting. According to Cassie`s equation, smaller area fraction of the vapor on the surface will lead to the decrease of contact angle.[24,25] Therefore, with the increase of Ni-W alloy deposition time, the air volume beneath the water droplet decreases,which lead to the decrease of contact angle. According to Nosonovsky and Bhushan's theory,[26] the hemispherical top is more desirable for maximum contact angles than cones since sharp edges may lead to pinning of triple line and the grooves may act as open capillaries to reinforce wetting. Besides, the spaces among the micro-hemispheres can hold more air pocket thus preventing the droplet from touching the valley between microcones. Fig.9 illustrates the contact modes of water droplets on two different micro-structured surfaces. This prominent property of films can be applied to self-cleaning and corrosion prevention.

4. Conclusions

In summary, the Cu MCAs / Ni-W alloy coating with a hemisphere top is fabricated by the employment of electroless and electro deposition. With different deposition times, the morphology can be modified and the related growth mechanism is studied. It shows superhydrophobicity with a water contact angle of 153.2°. The

hemispherical top of the micro-post avoids the pinning of triple line and plays an important role in superhydrophobicity. Tafel curve shows that the Cu MCAs coated Ni-W alloy film reveals the excellent anti-corrosion property. This research may enrich our understanding of the metallic materials and microstructures, which may have broad prospects in the fields like anti-wetting materials fabrications.

Acknowledgments

This work is sponsored by National Natural Science foundation of China (61176097, 61376107) and the National Basic Research Program of China (973 Program, 2015CB057200). We also thank the Instrumental Analysis Center of Shanghai Jiao Tong University for the use of the SEM/EDS equipment.

References

1. Y.-L. Zhang, H. Xia, E. Kim and H.-B. Sun, *Soft Matter*, 2012, **8**, 11217-11231.

2. F. Shi, J. Niu, J. Liu, F. Liu, Z. Wang, X. Q. Feng and X. Zhang, *Advanced Materials*, 2007, **19**.

3. F. Zhang, L. Zhao, H. Chen, S. Xu, D. G. Evans and X. Duan, *Angewandte Chemie International Edition*, 2008, **47**, 2466-2469.

4. T. Liu, Y. Yin, S. Chen, X. Chang and S. Cheng, *Electrochimica Acta*, 2007, **52**, 3709-3713.

5. L. Feng, Z. Zhang, Z. Mai, Y. Ma, B. Liu, L. Jiang and D. Zhu, *Angewandte Chemie International Edition*, 2004, **116**, 2046-2048.

6. Q. Wang, Z. Cui, Y. Xiao and Q. Chen, *Applied Surface Science*, 2007, **253**,

9054-9060.

7. M. Wang and H. Wang, *Applied Surface Science*, 2008, **254**, 6002-6006.

8. J. Drelich, E. Chibowski, D. D. Meng and K. Terpilowski, *Soft Matter*, 2011, **7**, 9804-9828.

9. R. Ramachandran and M. Nosonovsky, *Soft Matter*, 2014, **10**, 7797-7803.

10. X. Feng and L. Jiang, *Advanced Materials*, 2006, **18**, 3063-3078.

11. Y. Zhang, S. Wei, F. Liu, Y. Du, S. Liu, Y. Ji, T. Yokoi, T. Tatsumi and F.-S. Xiao, *Nano Today*, 2009, **4**, 135-142.

12. X. Mo, Y. Wu, J. Zhang, T. Hang and M. Li, *Langmuir*, 2015.

13. W. Zhang, Z. Yu, Z. Chen and M. Li, *Materials Letters*, 2012, **67**, 327-330.

14. R. Berriche, R. Lowry and M. I. Rosenfield, An oxidation study of Cu leadframes, 1999.

15. T. Yamasaki, R. Tomohira, Y. Ogino, P. Schlossmacher and K. Ehrlich, *Plating and Surface Finishing(USA)*, 2000, **87**, 148-152.

16. Y. Shacham-Diamand and Y. Sverdlov, *Microelectronic engineering*, 2000, **50**, 525-531.

17. W.-H. Hui, J.-J. Liu and Y.-S. Chaug, *Surface and Coatings Technology*, 1994, **68**, 546-551.

18. H. R. Kotadia, O. Mokhtari, M. Bottrill, M. P. Clode, M. A. Green and S. H. Mannan, *Journal of Electronic Materials*, 2010, **39**, 2720-2731(2712).

19. K. Sriraman, S. G. S. Raman and S. Seshadri, *Materials Science and Engineering: A*, 2006, **418**, 303-311.

20. F. Hu, H. Wang, S. Yang, A. Hu and M. Li, *Applied Surface Science*, 2015, **353**, 774-780.

21. W. Zhang, X. Feng, H. Cao, A. Hu and M. Li, *Applied Surface Science*, 2012, **258**, 8814-8818.

22. T. Yamasaki, *Scripta Materialia*, 2001, **44**, 1497-1502.

23. M. Obradovic, J. Stevanovic, A. Despic, R. Stevanoyic and J. Stoch, *JOURNAL-SERBIAN CHEMICAL SOCIETY*, 2001, **66**, 899-912.

24. R. N. Wenzel, *Industrial & Engineering Chemistry*, 1936, **28**, 988-994.

25. A. Cassie, *Discussions of the Faraday Society*, 1948, **3**, 11-16.

26. M. Nosonovsky and B. Bhushan, *Journal of Physics Condensed Matter*, 2008, **20**, 225009-225038.

Figures

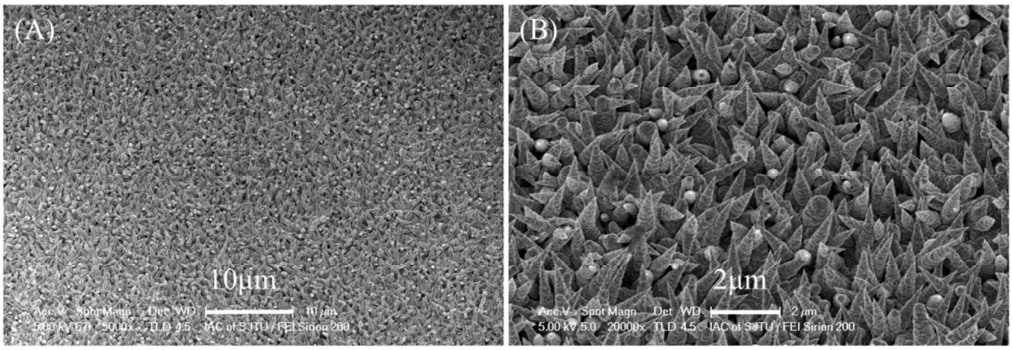

Fig.1 Low (A) and high (B) magnification SEM images of copper microcone arrayed structures surface.

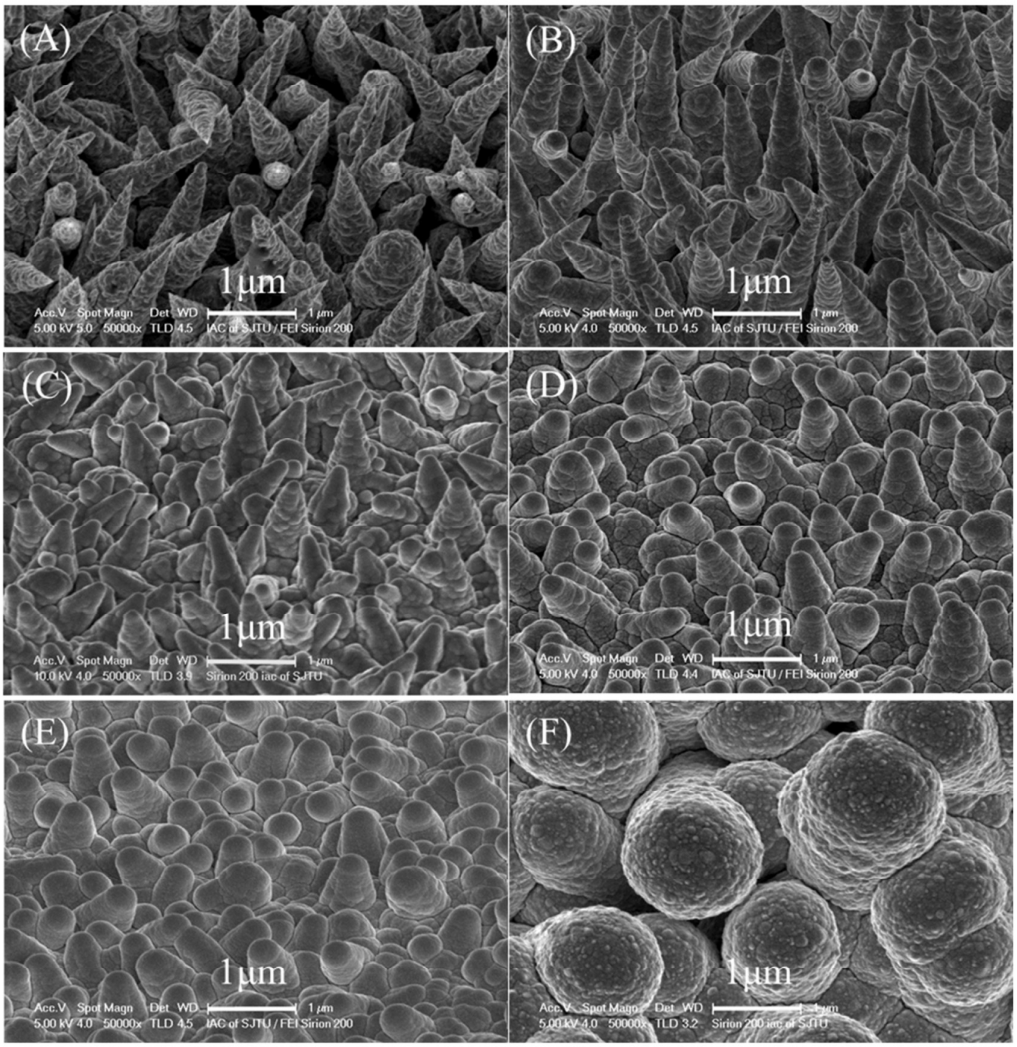

Fig. 2. SEM images of Cu MCAs surface after deposition of Ni-W alloy coating for (A) 0 min, (B) 0.5 min, (C) 1 min, (D) 1.5 min,(E) 2 min and (F) 2.5 min.

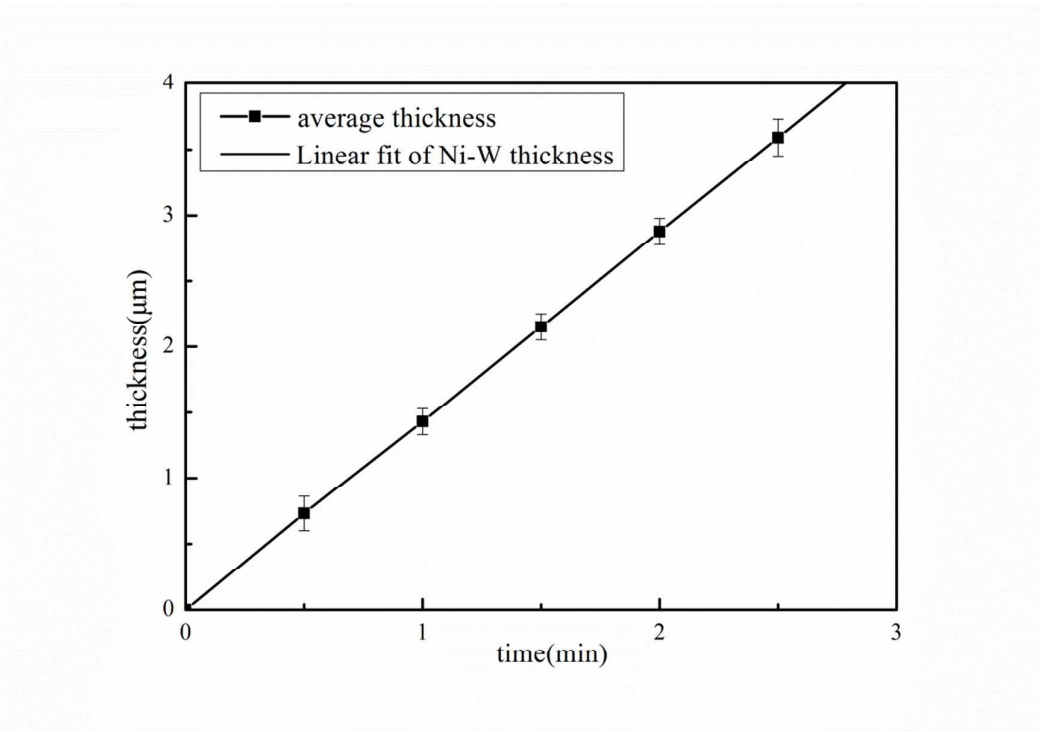

Fig.3. Thickness of Ni-W alloy coating with differentg plating time.

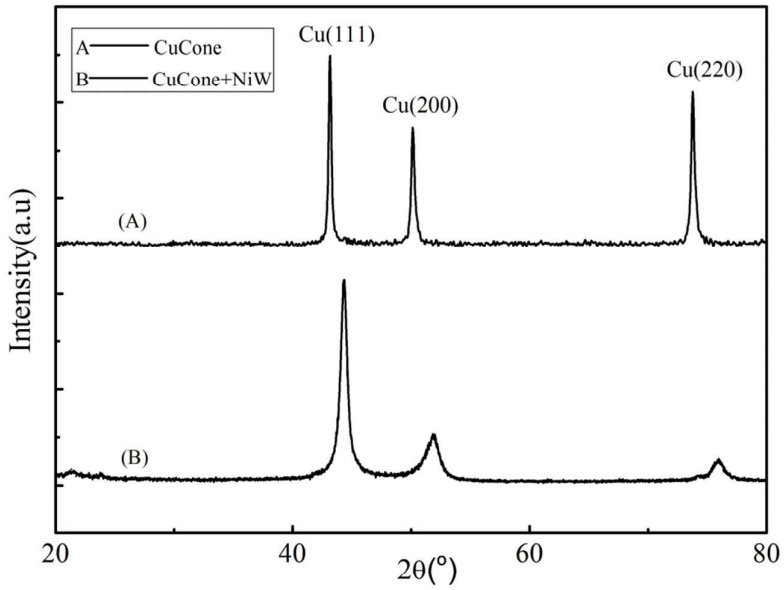

Fig. 4. XRD diffraction patterns of (A) Cu MCAs and (B) Cu MCAs with Ni-W(25 wt.%) alloy coating

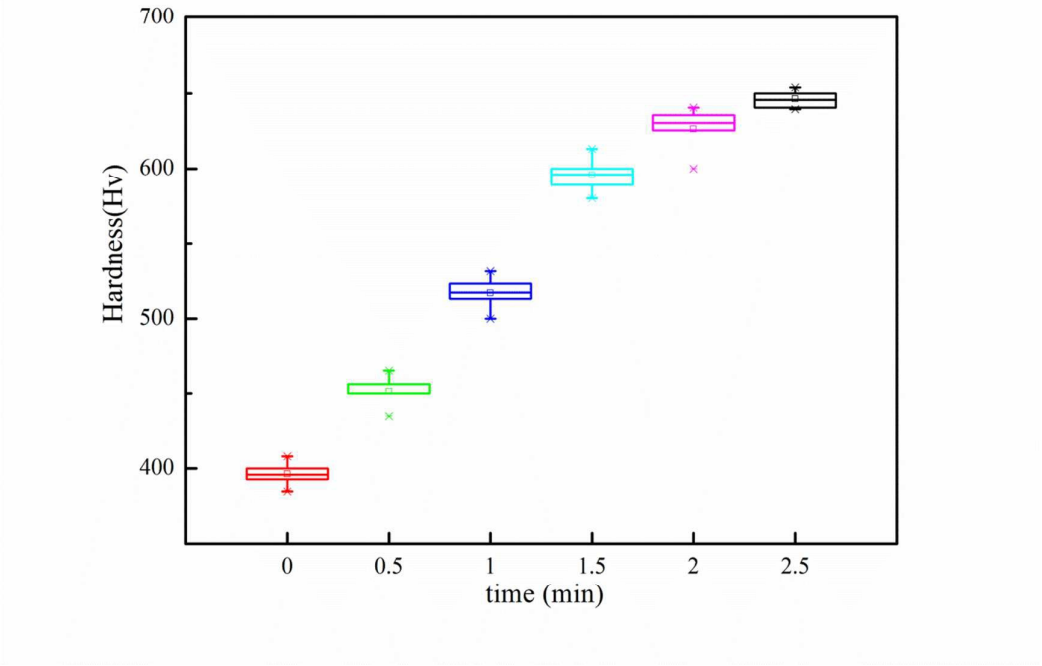

Fig.5. Hardness of Cu MCAs coated Ni-W coating varied plating time.

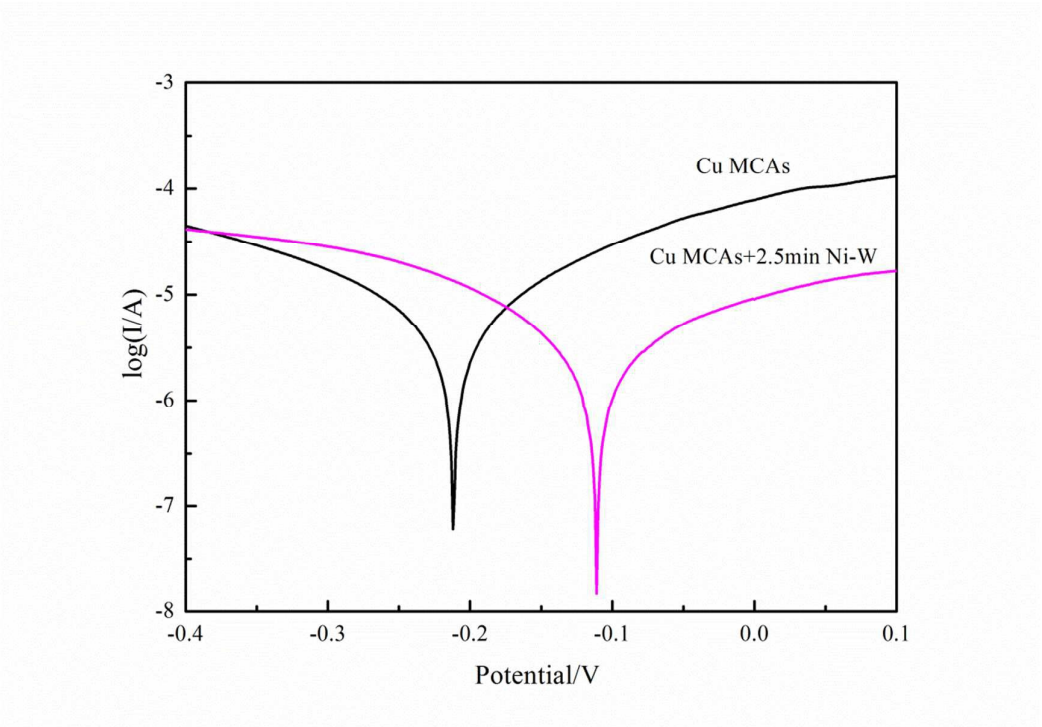

Fig.6. Tafel curves of CuMCAs and CuMCAs coated Ni-W alloy in 3.5 wt% NaCl solution.

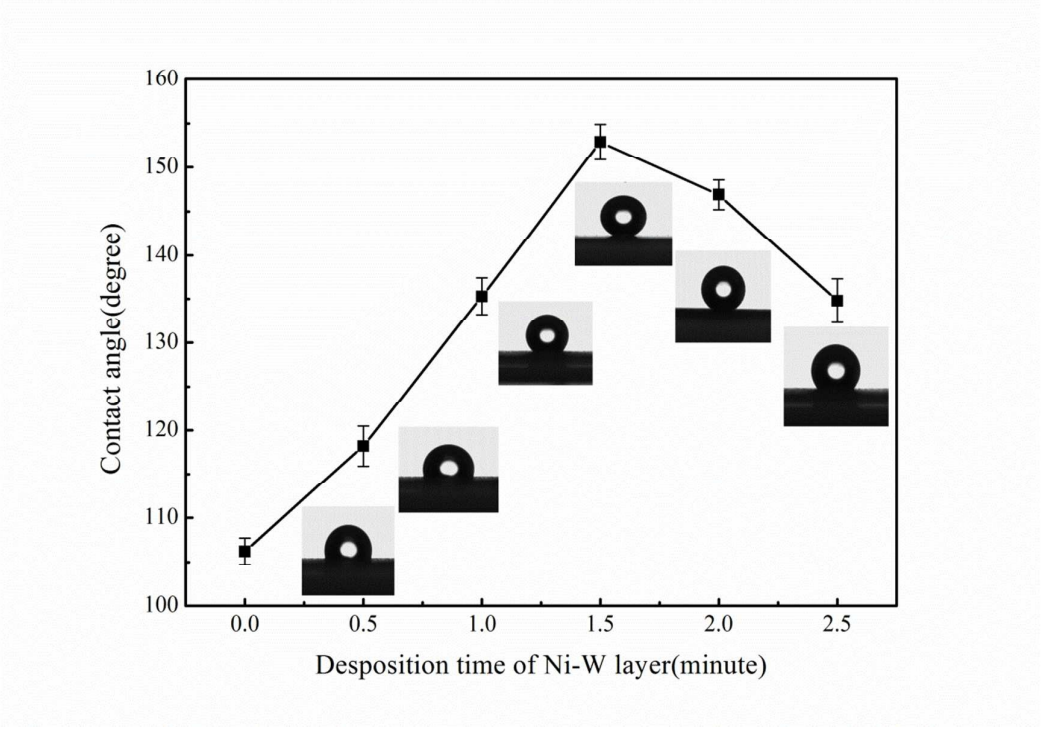

Fig. 7. Optical graphs of water droplets (3μL) on Cu MCAs / Ni-W alloy coating surface corresponding to the deposition time of Ni-W alloy.

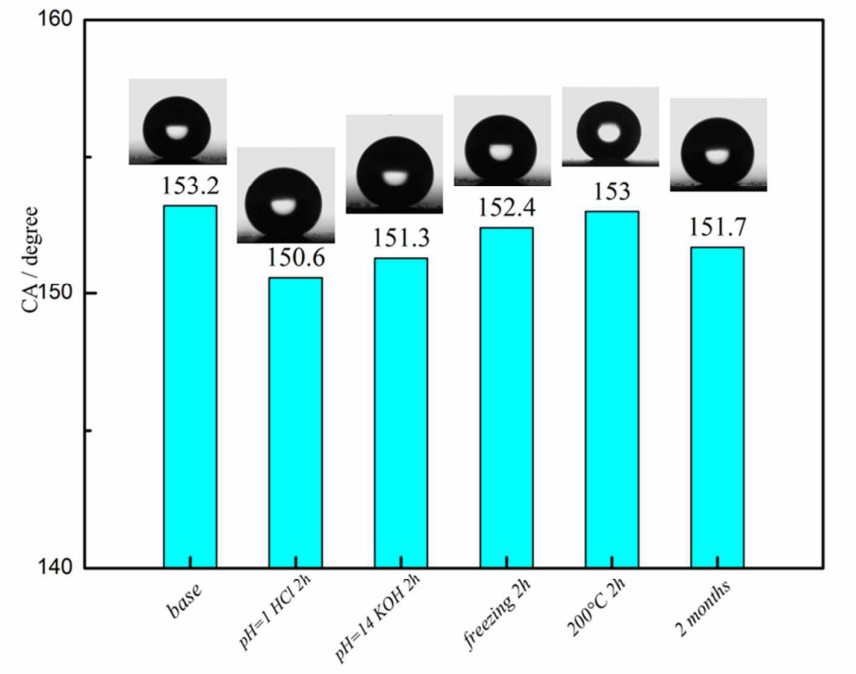

Fig.8. Contact angle of the superhydrophobic surface under different environment.

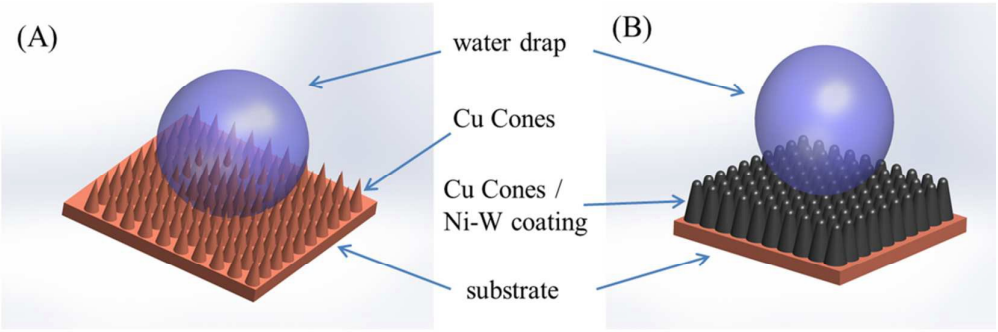

Fig.9. Schematics of two different wetting modes on (A) Cu MCAs and (B) Cu MCAs / Ni-W micro-posts arrayed structures.